

of the gradient term (or the x -dependent effective mass). Thus an alternative separation of v , which preserves the Mathieu character of the φ variable, would presumably still yield a similar node structure near $\theta=0$.

¹³Recently, we have learned of the specific-heat mea-

surements of A. Ramirez and W. P. Wolf. Here again the experimental results appear to agree much better with an effective sine-Gordon theory with a soliton mass smaller by about 20%. A detailed analysis of this experiment is in progress and will be added to Ref. 11.

Transient Optical Spectra of a Dense Exciton Gas in a Direct-Gap Semiconductor

G. W. Fehrenbach, W. Schäfer, J. Treusch, and R. G. Ulbrich

Institut für Physik der Universität Dortmund, 46 Dortmund 50, Federal Republic of Germany

(Received 26 July 1982)

The observation is reported of a remarkable persistence of the $1s$ exciton resonance in transient picosecond absorption spectra of GaAs under conditions of *resonant* optical excitation up to pair densities two orders of magnitude above the Mott density. The stability (excess linewidth < 0.8 meV at $n = 6 \times 10^{16}$ cm⁻³) of this dense exciton gas against decay into the energetically more favorable continuum of electron-hole pairs is due to the relatively weak self-screening of discrete excitons.

PACS numbers: 71.35.+z, 78.40.Fy

In 1968 Keldysh suggested that excitons—the lowest electronic excited states of semiconductors—might condense to a metallic phase at sufficiently high pair densities.¹ The insulating gas of bosonlike, strongly correlated electron-hole ($e-h$) pairs transforms with increasing density into a bipolar plasma of electrons and holes, which in turn—via metallic screening—destroys the long-range Coulomb interaction responsible for the formation of discrete excitons. According to Mott, excitons become unstable at an $e-h$ pair density n_M where the corresponding plasma screening length is comparable to the excitonic Bohr radius a_B .²

Meanwhile there is a wealth of knowledge on high-density excitons, $e-h$ liquids, and the Mott criterion for excitonic stability.³ The emphasis in experimental as well as theoretical work was given primarily to the *metallic* aspect of the excited system, and its *plasma screening* properties: Quasi cw edge absorption measurements in the direct-gap semiconductor GaAs with optical pumping above the band gap by Shah, Leheny, and Wiegmann⁴ and calculations by Zimmermann *et al.*⁵ confirmed the Mott criterion, which leads in the case of GaAs to a Mott density of $n_M = 5.4 \times 10^{14}$ cm⁻³ at $T = 0$. Transient experiments by Shank *et al.* have proven that the screening mediated through optically excited hot $e-h$ pairs (with excess energies of ~ 0.5 eV above E_g) is more or less instantaneous, even on a picosecond scale.⁶

In this Letter we report the first observation

of sharp, transient excitonic spectra in the direct-gap semiconductor GaAs under picosecond *resonant* $1s$ exciton pumping conditions up to pair densities n exceeding the Mott density n_M by two orders of magnitude. We propose a model and present calculations of exciton self-screening in this metastable state to explain the key features of the absorption spectra and its relative stability against decay into the $e-h$ pair continuum, which is—in thermal quasiequilibrium—energetically more favorable if $n \geq n_M$.

The GaAs samples of controlled thickness $t = 0.5$ and $t = 4.2$ μm were prepared by standard lapping, etching, and ion milling procedures from high-purity ($N_D, N_A \leq 2 \times 10^{14}$ cm⁻³) liquid-phase-epitaxy material. The samples were held freely between glass plates and immersed in liquid He at 1.2 K. Light pulses from a synchronously mode-locked dye laser were adjusted to 8-psec duration with a spectral width of 1.2 meV and tuned on the center of the $1s$ exciton resonance at 1.515 eV. The experiments were performed in excite-and-probe configuration, with adjustable delay Δt and continuously variable beam intensities of fixed ratio 100:1. Both beams were focused to 30- μm -diam spot size, sent at near perpendicular incidence through the sample, and analyzed with a 0.85-m double-grating spectrometer (resolution 0.1 meV) and a photomultiplier. The absolute excitation-pulse energies before the sample were measured with a calibrated, fast $p-i-n$ photodiode, and simultaneously the true

temporal behavior of the light pulses was measured with an autocorrelation setup. The deposited excitation-pulse energy and hence the actual pair density in the sample were determined directly from careful measurements of the incident, the reflected, and the transmitted excitation-pulse spectra and appropriate subtraction and integration over wavelength. Since all recovery time constants were much longer than 8 psec, it was straightforward to find—under the assumption of homogeneous excitation across the 0.5- μm sample thickness—the pair density n .

Figure 1 (lower trace) shows for reference the cw low-density absorption spectrum of an optically thick sample with the exciton Rydberg series up to $n=3$ and the onset of the continuum at the gap energy $E_g^{(0)}$. The corresponding spectrum of the ultrathin sample (Fig. 1, middle trace) shows a dominating and fully resolved $1s$ exciton resonance; the higher-lying discrete states have merged with the continuum because of their size. Typical transient probe absorption spectra at $\Delta t = 8$ psec are shown in Fig. 1 (top traces) for three different deposited pair densities n . The inset shows the temporal dependence of the probe absorption at fixed energy 1.515 eV and an excitation-pulse energy corresponding to $n = 6 \times 10^{16} \text{ cm}^{-3}$. All measured recovery times were longer than 30 psec (~ 100 psec in the wings of the resonance). The three key features observed are as follows: (i) the $1s$ exciton peak remains practically constant in energy up to $n = 2 \times 10^{17} \text{ cm}^{-3}$, (ii) the $1s$ exciton linewidth increases very little up to $2 \times 10^{16} \text{ cm}^{-3}$, (iii) its oscillator strength decreases above that density and the line profile develops a high-energy shoulder above $6 \times 10^{16} \text{ cm}^{-3}$. In Fig. 2 we have plotted the measured energetic positions (circles) and excess half-widths (vertical bars) of the $1s$ exciton line.

For a qualitative understanding of the experimental facts—sharp and unshifted exciton spectra up to densities of 2 orders of magnitude above n_M —we have to realize the fundamental difference between (i) plasma screening mediated through free $e-h$ pairs and (ii) nonmetallic (or “dielectric”) excitonic screening which is caused by the very existence of the excitons themselves. If only $1s$ excitons are created by means of pulsed optical excitation the plasma screening process is initially not effective. This holds for times short compared with the inelastic scattering time within the exciton system, i.e., the onset of exciton ionization via multiple inelastic exciton scattering and subsequent creation of continuum $e-h$

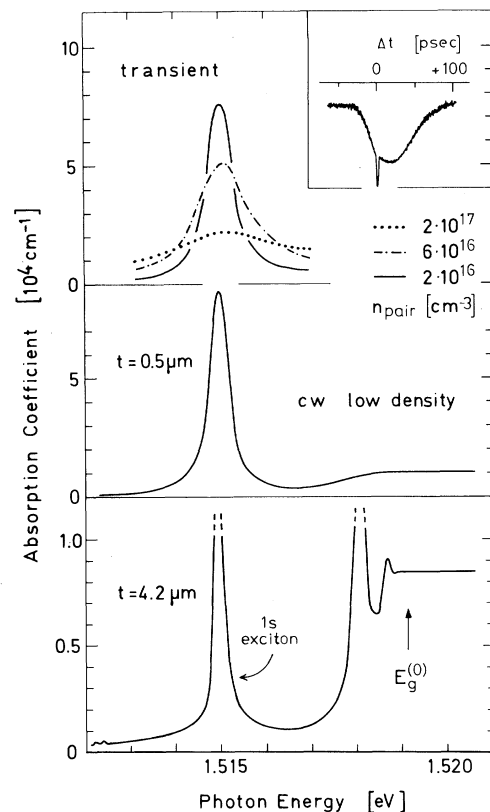


FIG. 1. Transient optical absorption spectrum of an ultrathin GaAs platelet under conditions of simultaneous resonant excitation with 8-psec light pulses of 1.2-meV spectral half-width centered on the $1s$ exciton line at three different instantaneous pair densities (top three traces). Inset: Temporal behavior of the probe-beam absorption coefficient for fixed photon energy 1.515 eV after deposition of $6 \times 10^{16} \text{ cm}^{-3}$ pair density by the excitation pulse. The width of the sharp spike at $\Delta t = 0$ indicates the coherence time of the laser pulse (coherence time). The quoted transient probe absorption spectra were taken at $\Delta t = 8$ psec. For comparison the corresponding cw low-density spectra are shown for the same sample (middle) and an “optically thick” sample of the same crystal quality (bottom).

pairs. In the case of exciton screening a given exciton interacts with the externally excited $1s$ exciton gas, a long-range polarizable medium.⁷ The corresponding screening function does not diverge for $\omega = 0$ and $q \rightarrow 0$, in contrast to plasma screening. This is a consequence of the gap of $\sim \frac{3}{4}$ exciton rydberg in the excitation spectrum of the real exciton gas. A difficulty encountered here is the fact that the polarizability is caused by the excitons themselves: The interaction potential entering the effective exciton equation depends on the exciton energy, and therefore dynamical screening effects are crucial.

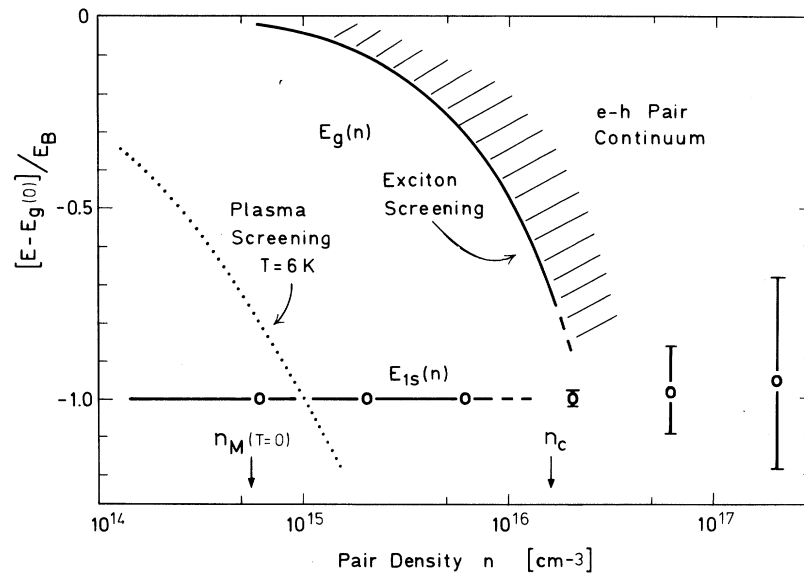


FIG. 2. Experimentally determined peak positions (circles) and excess half-widths (vertical bars) of the 1s exciton absorption structure for six different pair densities n . The horizontal full line gives the calculated 1s exciton energy as a function of exciton density. The theoretical dependence of the continuum edge $E_g(n)$ on exciton (respectively, pair) density is shown for the exciton screening mechanism (full curve) and also for plasma screening (dotted curve, taken from Ref. 5). Mott density n_M and the critical density n_c (see text) are indicated.

We present here briefly the results of a variational calculation of the 1s exciton energy and a calculation of the shift of the continuum edge, assuming that only 1s excitons of density n are present at $T=0$. We neglected all multiple exciton scattering processes, phonon scattering, and radiative recombination, since the corresponding relaxation times are long compared with the picosecond time scale considered here. Then the effective interaction entering the Bethe-Salpeter equation is

$$V = V_0 + V_0 \chi_{ex} V_0, \quad (1)$$

where $V_0(q) = 4\pi e^2 / \epsilon_0 q^2$ is the statically screened Coulomb interaction entering the zero-density equation. The additional density dependent polarizability is

$$\chi_{ex}(q, \omega; n) = n \sum_{\nu > 1, lm} |\langle 1s | e^{i\mathbf{q}\cdot\mathbf{r}} | \nu lm \rangle|^2 \times \left(\frac{1}{E_{1s} - E_\nu - \hbar\omega} + \frac{1}{E_{1s} - E_\nu + \hbar\omega} \right) \quad (2)$$

which describes virtual transitions between the populated 1s exciton state at energy E_{1s} and excited exciton states $|\nu lm\rangle$. An effective, dynamically screened exciton Hamiltonian H_{eff} can now be derived in the so-called Shindo approximation,⁸ originally used in the field of exciton-phonon

coupling and then adopted in the theory of plasma screening.⁵ In addition to the usual hydrogenic part including V_0 , H_{eff} contains a dynamic self-energy part and an induced interaction potential. The ground-state energy of H_{eff} , the 1s exciton energy, is calculated as its expectation value with 1s-type wave functions, and minimized with respect to their Bohr radius a_B . The parameters for GaAs were $m_e = 0.07m_0$, $m_h = 0.5m_0$, and $\epsilon_0 = 12.6$.⁹ We find that up to $n = 8 \times 10^{15} \text{ cm}^{-3}$ the contribution of the dynamical self-energy and the induced potential cancel to better than 1% of the unperturbed binding energy E_B^0 , in excellent agreement with experiment (see Fig. 2, horizontal full line). From the same Hamiltonian H_{eff} we calculate the continuum edge which—as it should be—equals the effective energy gap in the one-particle spectrum. This effective gap is shrunk as a result of the excitonic screening mechanism. In the case of GaAs we find

$$E_g(0) - E_g(n) = 35.1 a_B^3 n E_B^0 \quad (3)$$

with $a_B = 110 \text{ \AA}$.⁹ The calculated continuum-edge shift (Fig. 2, full curve) shows that the effective exciton binding energy vanishes at $n = 2.1 \times 10^{16} \text{ cm}^{-3}$, a density about 40 times larger than the Mott density. As a critical condition for the very existence of sharp excitonic structure in the opti-

cal spectrum we define here the density n_c where the actual exciton binding energy is reduced by such an amount that the spectral width of the excitation light pulse (1.2 meV) overlaps the continuum edge and directly creates free $e-h$ pairs, which in turn act as a plasma and screen the exciton, effectively. From inspection of Eq. (3) we deduce $n_c = 1.6 \times 10^{16} \text{ cm}^{-3}$, somewhat below the density where the experimental spectra begin to broaden considerably (see Fig. 2). If we had taken into account the kinetic energy of the 1s excitons in Eq. (2), the calculated critical density would be larger.

In conclusion, we have demonstrated the existence of a nonequilibrium exciton phase in GaAs up to densities exceeding the Mott density by two orders of magnitude. We show that the short-time behavior of resonantly excited 1s excitons is controlled by the polarizability of the exciton gas and not by plasma screening. Our results renew the question whether $e-h$ correlation is incorporated properly in existing descriptions^{3,5} of the quasiequilibrium ground state of $e-h$ pairs in the intermediate density regime, where until now the main emphasis was laid on the metallic as-

pect of screening.

¹L. V. Keldysh, in *Proceedings of the International Conference on the Physics of Semiconductors, Leningrad, 1967*, edited by S. M. Ryvkin and Yu. V. Shmartsner (Nauka, Leningrad, 1968), p. 1303.

²N. F. Mott, *Metal Insulator Transitions* (Taylor & Francis, London, 1974).

³For recent reviews, see T. M. Rice, *Solid State Physics* (Academic, New York, 1971), Vol. 32, p. 1; J. C. Hensel, T. G. Phillips, and G. A. Thomas, *ibid.*, p. 88; E. O. Göbel and G. Mahler, *Festkörperprobleme: Advances in Solid State Physics* (Vieweg, Braunschweig, 1979), Vol. XIX, p. 109; C. Klingshirn and H. Haug, *Phys. Rep.* **70**, 315 (1981).

⁴J. Shah, R. F. Leheny, and W. Wiegmann, *Phys. Rev. B* **16**, 1577 (1977).

⁵R. Zimmermann, K. Kilimann, W. D. Kraeft, D. Kremp, and G. Röpke, *Phys. Status Solidi (b)* **90**, 175 (1978).

⁶C. V. Shank, R. L. Fork, R. F. Leheny, and J. Shah, *Phys. Rev. Lett.* **42**, 112 (1979).

⁷This problem is similar to that of Fröhlich exciton-phonon coupling with equal exciton and polaron radii.

⁸K. Shindo, *J. Phys. Soc. Jpn.* **29**, 287 (1970).

⁹D. D. Sell, S. E. Stokowski, R. Dingle, and J. V. D'Iorio, *Phys. Rev. B* **7**, 4568 (1973). The parameter m_h was chosen to be equal to the average heavy-hole mass, and gives an effective Bohr radius of 110 Å.

Infrared Spectroscopy of Phonons in Hexagonal-Phase Solid Hydrogen

Chien-Yu Kuo, Martha M. F. Vieira,^(a) and C. K. N. Patel

Bell Laboratories, Murray Hill, New Jersey 07974

(Received 21 June 1982)

The pulsed-laser piezoelectric-transducer optoacoustic spectroscopy is used to study phonons in hexagonal-phase solid normal hydrogen. At temperatures of ~ 11 K, the phonon excitations associated with double-molecular transitions are predominantly transverse-optical phonons, whereas the excitations associated with single-molecular transitions are predominantly longitudinal-optical phonons. The LO phonon density of states is obtained for the first time.

PACS numbers: 78.30.Gt, 67.80.Cx, 78.20.Hp

The advent of the high-sensitivity technique of detecting weak absorptions in solid hydrogen utilizing the pulsed-laser piezoelectric-transducer (PULPIT) optoacoustic spectroscopy has enabled the study of overtone absorptions in solid hydrogen.¹ We report in this Letter the observation and analysis of TO and LO phonons associated with these overtone vibrational-rotational molecular transitions in solid normal hydrogen. In addition to the TO and LO phonon frequencies, we also obtain the respective density of states for

the two phonons.

Phonon frequencies and phonon density of states in solid hydrogen have been measured by several different techniques. These include Raman scattering and neutron scattering. Silvera and Hardy² have reported on an extensive Raman scattering study. Momentum conservation, in general, restricts the phonon studies using Raman spectroscopy to zone-center phonons for first-order processes. Fleury and McTague's elegant Raman scattering studies³ have, however, shown that the